Rhizoma alismatis polypeptide treats inflammatory bowel disease in mice by regulating immune balance

Zhongmei He[1], Tianyuan Liu[1], Rui Du[1], Xiaowei Dai[2], Honyan Pei[1], Qiaobing Guan[3], Shuiliang Ruan[3], Shasha Wu[3]

[1]College of Chinese Medicinal Materials, Jilin Agricultural University, Changchun 130118, China
[2]The Second Norman Bethune Hospital of Jilin University, Changchun 130118, China
[3]The Second Affiliated Hospital of Jiaxing University, Jiaxing 314001, China

Correspondence to: Shasha Wu; **email:** wushasha8383@126.com, https://orcid.org/0000-0002-8819-4246
Keywords: rhizoma alismatis polypeptide, colitis, regulatory T cell, immune balance
Received: September 4, 2023   **Accepted:** November 7, 2023   **Published:**

ABSTRACT

Aim: We isolated and identified RAP1, an active polypeptide in Rhizoma Alismatis, and investigated its anti-inflammatory mechanism.

Methods: Chronic colitis was induced in mice by dextran sulfate sodium (DSS). After RAP1 intervention, the life status, body weight and pathological score of mice were measured. The proportions of regulatory T cells (Treg), helper T cells 1 and 17 (Th1 and Th17) in mesenteric lymph nodes and spleen were determined by flow cytometry (FCM). Cytokine levels were detected by enzyme-linked immunosorbent assay (ELISA), and protein expressions were assayed by Western-Blotting.

Results: RAP1 improved the immune balance, increased the proportion of Tregs, while decreased the proportions of Th1 and Th7 cells. Meanwhile, it could lower the levels of inflammatory cytokines, ameliorate the chronic colitis and reduce the tissue inflammation and permeability.

Conclusions: RAP1 can inhibit tissue inflammation in chronic colitis by regulating intestinal immune balance, which is one of its mechanisms.

INTRODUCTION

Rhizoma Alismatis is the dried tuber of *Alisma orientalis* in the *Alismataceae* family. To date, over 220 compounds have been isolated from Rhizoma Alismatis, including triterpenes, sesquiterpenes, diterpenes, saccharides, nitrogen-containing compounds, phenylpropanoids, flavonoids and steroids [1]. Pharmacological studies have shown that the ethanol, aqueous extracts and some monomer components of Rhizoma Alismatis possess diuretic, antilithic, renal protective, hypolipidemic, hepatoprotective, hypoglycemic, anticancer, antioxidant, anti-inflammatory and anti-complement effects [2, 3]. The ethanol and aqueous extracts, along with many monomer components of Rhizoma Alismatis have an anti-inflammatory action. Apart from inhibiting cytokine activation and inflammatory mediator hyperplasia, the ethanol extracts can also suppress emphysema, weaken pulmonary fibrosis, and promote the expressions of inflammatory cytokines TNF-α, IL- by reducing pneumonic cell infiltration [4]. Moreover, they can reduce acute lung injury and inhibit lung infection in mice by suppressing the expressions of NF-κB and related genes and activating Nrf2 [5]. Extant research focuses on the activity of small monomer molecules, while the isolation and activity of polypeptides from Rhizoma Alismatis have scarcely been studied. Hence, there is a broad space for exploring the role of Rhizoma Alismatis polypeptides.

Chronic colitis is a common inflammatory disease, and the functional imbalance of immune cells is the major factor in the pathogenesis of colitis [6]. Imbalance of

immune Tregs and proinflammatory Th1/Th17 cells and substantial expression of inflammatory cytokines result in the progression of colitis [7–9]. Through isolation, we identified a Rhizoma Alismatis polypeptide and named it RAP1. In this study, we investigated the anti-inflammatory effect and mechanism of RAP1 with a mouse colitis model.

MATERIALS AND METHODS

Isolation and identification of RAP1

Total polypeptide of Rhizoma Alismatis (purity: >90%) provided by Walter Rice Biotechnology (Lanzhou, China) was used herein, which was a water-soluble polypeptide in a white powdery form. The polypeptide was dissolved and then isolated by high-performance liquid chromatography (HPLC) after ultrafiltration, ultimately yielding a novel polypeptide defined as RAP1.

Amino acid composition of RAP1: RAP1 was hydrolyzed by HCl to obtain free amino acids. Composition of the amino acids was analyzed with L-8900 amino acid analyzer (Hitachi, Japan). Initially, 100 mg of RAP1 and 9 mL of 6M HCl were mixed in ampoule tube, filled with nitrogen, sealed and kept at 110° for 24 h, followed by drying with nitrogen. Analysis was performed by post-column ninhydrin derivatization and UV detection.

Molecular weight distribution of RAP1: An Agilent 1100 HPLC system was adopted for determining the RAP1 molecular weight distribution. All standards utilized included aprotinin (6,511.51 Da), bacitracin (1,422.69 Da), glutathione oxidised (612.63 Da) along with glutathione reduced (307.32 Da). Blue dextran (2,000 kDa) was utilized to measure column void volume. After dissolving into deionized water at 2 mg/mL, the polypeptide was subjected to elution using 20 mM phosphate buffer that contained 0.15 M NaCl (pH 7.0) at the injection volume and flow rate of 5 μL and 0.25 mL/min, respectively.

Establishment of a mice model of chronic colitis

SPF-grade C57BL/6 mice aged 6–8 weeks, with body weights of (20±2) g, were reared in the Laboratory Animal Center of Jilin Agricultural University. Thirty mice were randomized into 3 groups, namely Control, DSS and RAP1. Mice colitis model was established by feeding the DSS and RAP1 groups with 3% DSS for 7 consecutive d [9, 10]. Mice in the Control group were fed with drinking water. The RAP1 group was also given tail vein injection of 10 mg/kg RAP1 once daily.

Physiological status and score of mice

During the experimentation, the physiological status, activity and mental state of mice were observed every day, and the changes in their body mass were recorded. From the 3rd d of model establishment, mice feces were collected to observe the fecal traits, and blood in feces was detected and recorded. The disease activity index (DAI) score was calculated as: DAI= (body mass loss score + fecal trait score + blood in feces score) /3.

On the 11th d of experimentation, after euthanizing the mice as per the relevant animal ethics requirements, the spleen and thymus tissues were dissected, carefully stripped, weighed and recorded for wet mass. The computational formula for spleen (thymus) index = wet mass of spleen (thymus) (mg)/body mass (g) × 10. The mouse mesenteric lymph nodes and colon tissues were separated, and colon length was measured. The mouse distal colon (~1 cm) was taken and fixed in 4% paraformaldehyde for 48 h.

Enzyme-linked immunosorbent assay (ELISA)

Appropriate amount of colon tissues was taken from mice, homogenized with normal saline (60 Hz, 120 s), and centrifuged (120,000×g) at 4° C for 10 min, followed by collection of homogenate supernatant. The levels of TNF-α, IL-1β, IL-6, IL-17A, TGF-β and IFN-γ were determined strictly following the ELISA kit instructions. All of the TNF-α, IL-1β, IL-6, IFN-γ, IL-17A and TGF-β assay kits were purchased from Meimian Industrial (Jiangsu).

Flow cytometry (FCM)

Fresh mesenteric lymph node and spleen tissues of mice were collected and mechanically ground. The spleens were additionally added with RBC lysis buffer to prepare cell suspension. Each tube was separately added with CD3 (PE/CY7, 1 μL per tube), CD4 (FITC, 1 μL per tube) and CD25 (APC, 1 μL per tube) antibodies at 10^6 cells. Besides, negative and single stained tubes were also prepared. After 30 min of incubation at room temperature away from light, the cells were washed twice with PBS, and subjected to membrane rupture with working solution (900 μL per tube) for 30 min away from light, followed by twice washing with fixed solution. Next, each tube was separately added with IFN-γ (APC, 3 μL per tube), IL-17A (BV421, 1 μL per tube) and Foxp3 (PE, 3 μL per tube) antibodies, and incubated at room temperature for 30 min away from light. Thereafter, the cells were washed twice with PBS, resuspended with 300 μL of PBS and analyzed for the Th1, Th17 and Treg cell proportions in mesenteric lymph node

and spleen tissues by FCM. The Mouse-PE/cyanine7-anti-CD3, Mouse-FITC-anti-CD4, Mouse-APC-anti-CD25, Mouse-APC-anti-IFN-γ, Mouse-PE-anti-Foxp3 and Mouse-BV421-anti-IL-17A antibodies were all purchased from BioLegend (USA).

Western-blotting

For tissue protein detection, liquid nitrogen homogenate was extracted from mouse intestinal tissues, and lysed on ice with 1.0 ml of precooled RIPA buffer (Beyotime Biotechnology, Shanghai, China) for 30 min. Protein quantification was performed by BCA assay and the protein concentration was adjusted. After denaturation at 100ºC, the protein fluid was electrophoresed and transferred onto the membranes, followed by membrane blockade with 5% skim milk powder. Thereafter, the membranes were incubated at 4ºC overnight with monoclonal antibody (1:450 dilution in TBST), washed with TBST, and further incubated with HRP-labeled secondary antibody (Abcam, USA) for 2 h. Chemiluminescence assay was performed, and optical density was analyzed via the Image Pro-Plus 6.0. The results were expressed as the optical density comparisons between the target protein and the GAPDH internal reference. The Mouse-ZO1, Mouse-Occludin, Mouse-FOXP3, Mouse-IFN-γ and Mouse-IL-17A antibodies were all purchased from Abcam (USA).

Statistical methods

Data were analyzed by SPSS 20.0, and mapped with the aid of GraphPad Prism 8.0. Measurement data were expressed as x ± SD. For measurement data conforming to normal distribution with homogeneous variance, one-way ANOVA was adopted for multi-group comparison, while LSD test was employed for pairwise comparison. As for those conforming to normal distribution with heterogeneous variance, Dunnett's T3 test was adopted. $P < 0.05$ was considered statistically significant.

Availability of data and material

The data that support the findings of this study are available from the corresponding author upon reasonable request.

Consent for publication

All authors approval published the article

RESULTS

Identification of RAP1

Amino acid analysis revealed that RAP1 contained Asp, Thr, Ser, Glu, Gly, Ala, Cys, Val, Met, Ile, Leu, Tyr, Phe, Lys, NH3, His, Arg, etc. According to the molecular weight distribution results of RAP1, Mp 1014, Mn 637, Mw 995, Mz 1688, Mv 922 kD (Figure 1 and Table 1).

Effects of RAP1 on life and pathological score in colitis mice

Dynamic weight detection revealed that the weight of Control mice increased slightly, while DSS could induce weight loss, and RAP1 could slow down the weight loss trend, showing significant difference from the DSS group at identical time points (Figure 2A). DAI
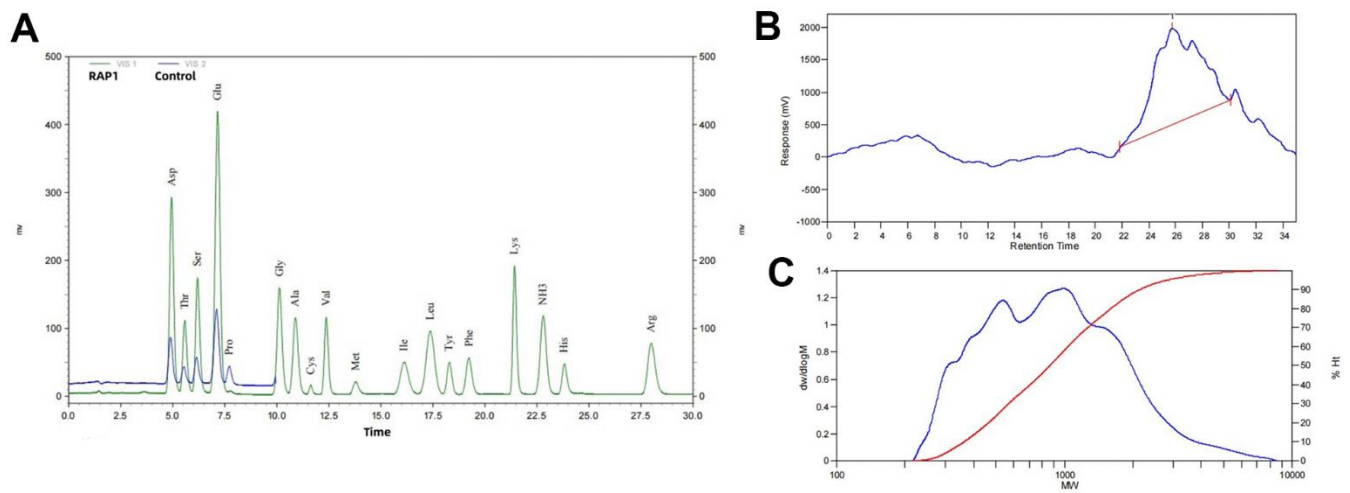

Figure 1. RAP1 identification results. (**A**) Amino acid composition and HPLC spectrum. (**B**, **C**) Molecular weight distribution analyses.

Table 1. Amino acid composition of RAP1.

| Amino acids	RT	Conc/ng	ESTD Conc/nmol
Asp	4.947	1235.520	9.283
Thr	5.580	365.672	3.070
Ser	6.193	530.940	5.052
Glu	7.160	2435.730	16.558
Gly	10.127	423.758	5.654
Ala	10.900	387.947	4.467
Cys	11.627	79.183	0.330
Val	12.373	383.021	3.271
Met	13.793	120.054	0.805
Ile	16.120	396.173	3.020
Leu	17.380	788.199	6.008
Tyr	18.293	325.188	1.795
Phe	19.237	362.414	2.194
Lys	21.427	595.876	4.076
NH3	22.800	68.196	4.004
His	23.820	222.229	1.432
Arg	27.997	751.730	4.315
			75.323
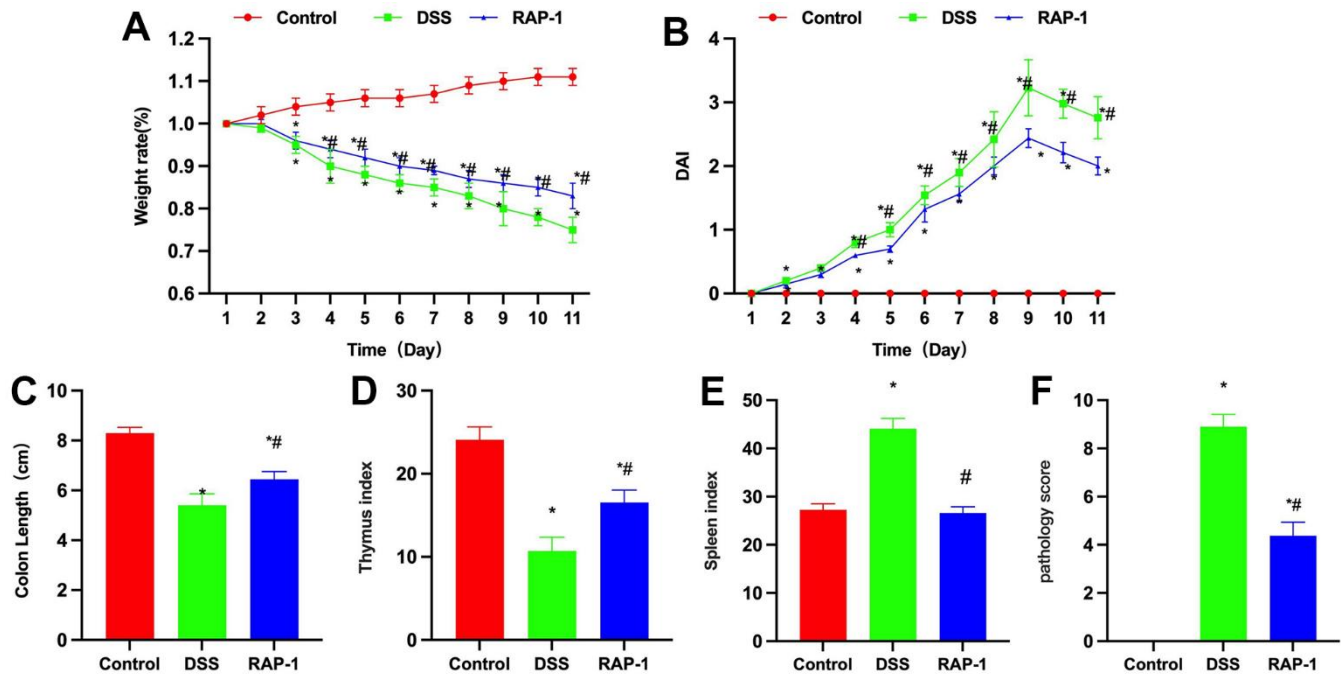
Figure 2. Effects of RAP1 on life and pathological score in colitis mice. (**A**) Dynamic weight monitoring (n= 10). DSS could induce weight loss in mice, while RAP1 could slow down such weight loss trend. (**B**) DAI scoring (n= 10). DSS mice exhibited increase in the DAI score. RAP1 mice displayed significantly lower DAI score than the DSS mice, albeit certain increase. (**C**) Intestinal length measurement (n= 10). Intestinal length was shortened in the DSS group, which was shorter than that in the RAP1 group. (**D, E**) Thymus and spleen indices (n= 10). DSS group exhibited lower thymus index and higher spleen index than the Control group. RAP1 could heighten the thymus index and lower the spleen index. (**F**) Pathological scoring (n= 10). Control mice scored 0, while significant score reduction was noted in the RAP1 group, showing lower value than the DSS group. *P< 0.05 vs. Control; #P< 0.05 vs. DSS.

scoring revealed that the score of Control mice was 0, where the pathological changes were unobvious. The DSS mice exhibited elevation in the DAI score. Although DAI score of RAP1 mice was heightened, it was significantly lower than that of DSS mice (Figure 2B). Intestinal length measurements showed shortened intestinal length in the DSS group, which was shorter than that of RAP1 group (Figure 2C). According to the measurements of thymus and spleen indices, the DSS group exhibited lower thymus index and higher spleen index than the Control. RAP1 could heighten the thymus index and reduce the spleen index (Figures 2D, 2E). Pathological scoring demonstrated that the Control group scored 0, while RAP1 could significantly reduce the score, showing lower value compared to the DSS group (Figure 2F).

Effects of RAP1 on inflammatory cytokine expressions

DSS could induce tissue inflammation, leading to upregulations of IL-1β, IL-6 and TNF-α in intestinal tissues. Besides, the levels of Th17 cell marker IL-17A and Th1 cell marker IFN-γ were upregulated, while the level of TGF-β1 was downregulated. RAP1 could

reduce the expressions of inflammatory cytokines and elevate the level of TGF-β1 (Figure 3).

Effects of RAP1 on immune cell balance

The proportions of Th1, Th17 and Treg cells in mesenteric lymph nodes and spleen were determined. We found upregulated Th1 proportions in mesenteric lymph nodes and spleen among the DSS mice, which were higher than those among the Control mice. RAP1 could reduce the Th1 proportion (Figures 4A). Similarly, the DSS group also exhibited higher Th17 proportion in mesentery and spleen than the Control group, while RAP1 reduced the Th17 proportion (Figures 4B). The Treg proportions in mesentery and spleen were lower in the DSS group than in the Control, while RAP1 increased the Treg proportion (Figures 4C).

Relative protein expressions

Our detection of protein expressions found that compared to the Control group, the levels of tight junction proteins ZO-1, Occludin and FOXP3 decreased in the DSS group, while the levels of IL-17A and IFN-γ
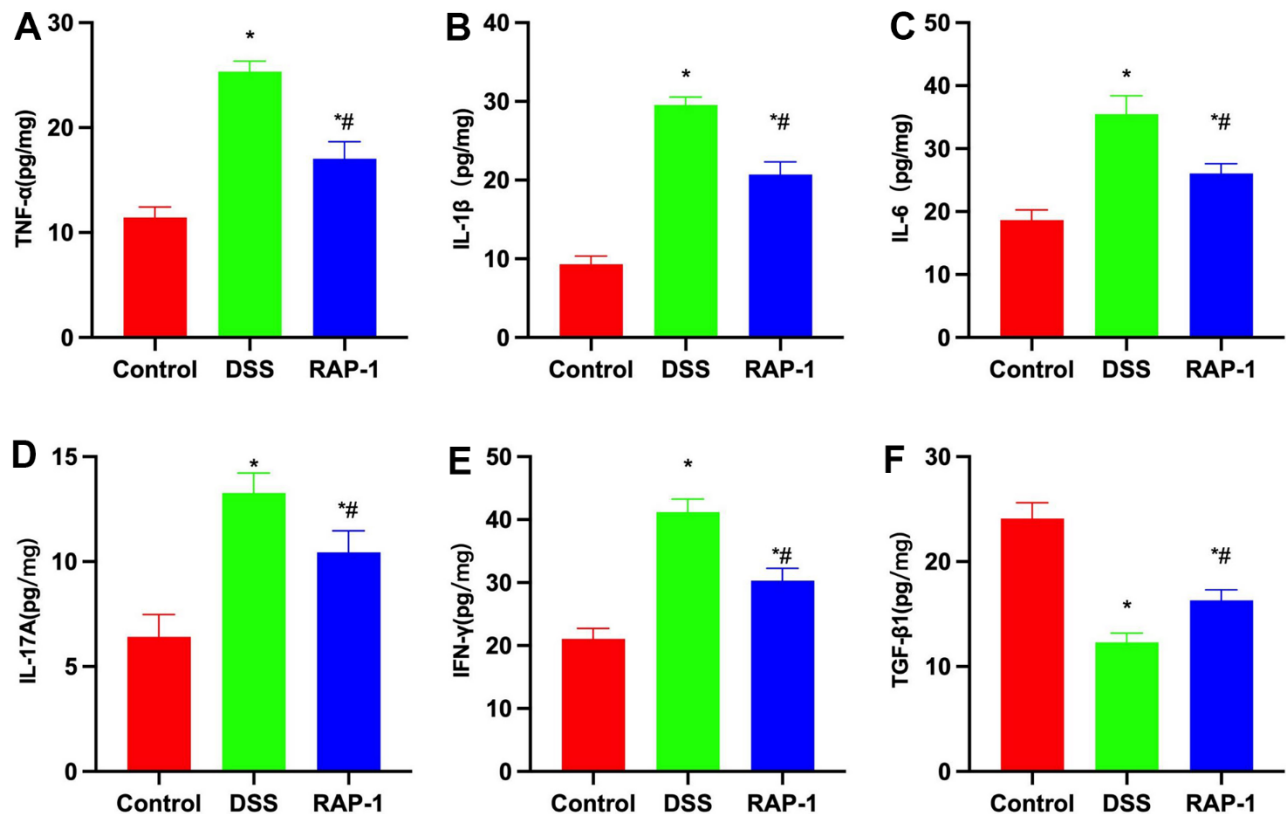
Figure 3. Changes in inflammatory cytokine expressions (n= 10). (**A–F**) RAP1 could lower the tissue levels of inflammatory cytokines and elevate the TGF-β1 level. *P< 0.05 vs. Control; #P< 0.05 vs. DSS.

increased. RAP1 could elevate the ZO-1, Occludin and FOXP3 levels and reduce the IL-17A and IFN-γ levels (Figure 5A–5F).

DISCUSSION

Chronic colitis is a common inflammatory disease. After its induction in animal model with 3% DSS, the body mass of model mice decreased, symptoms like diarrhea and rectal hematochezia appeared, DAI score rose significantly, and colon length was evidently shortened. Pathological observation showed occurrence of acute mucosal injury in colitis mice, as well as infiltration of colitis tissue mucosal layer and submucosa by inflammatory cells. Due to the influence of DSS on the bodily immune system, there were
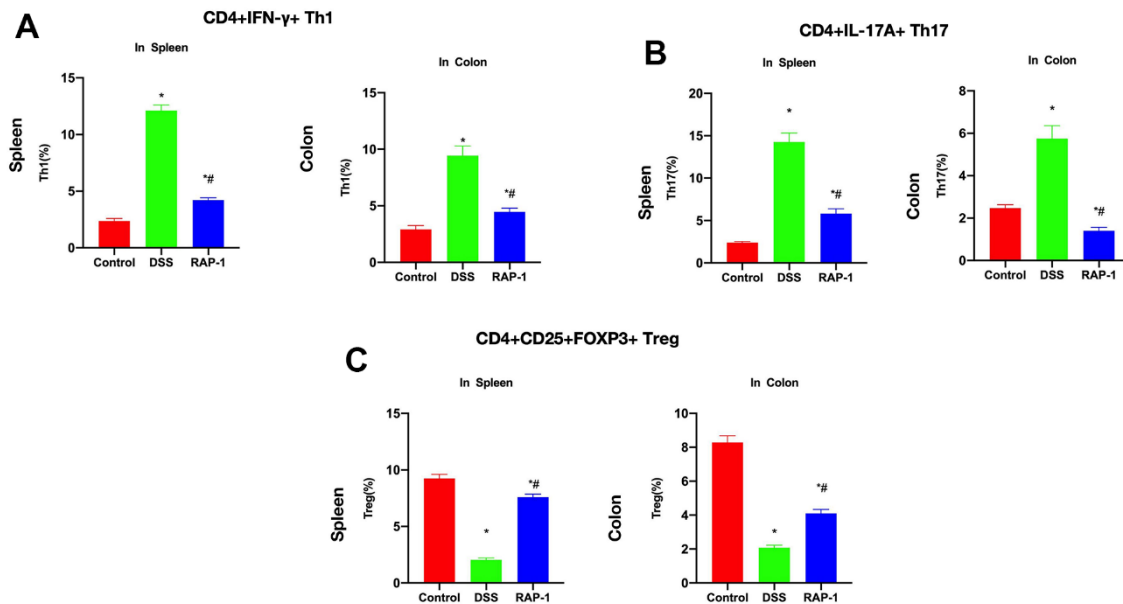

Figure 4. Immune lymphocyte assay results. (**A**) Th1 cells (n= 10). The Th1 proportions in mesenteric lymph nodes and spleen were upregulated in DSS group, which were higher than those in Control. RAP1 could lower the Th1 proportion. (**B**) Th17 cells (n= 10). The Th17 proportions in mesentery and spleen were also higher in the DSS group than in the Control, and RAP1 reduced the Th17 proportion. (**C**) Treg cells (n= 10). DSS group exhibited lower Treg proportions in mesenteric lymph nodes and spleen compared to Control, and RAP1 increased the Treg proportion. *P< 0.05 vs. Control; #P< 0.05 vs. DSS.
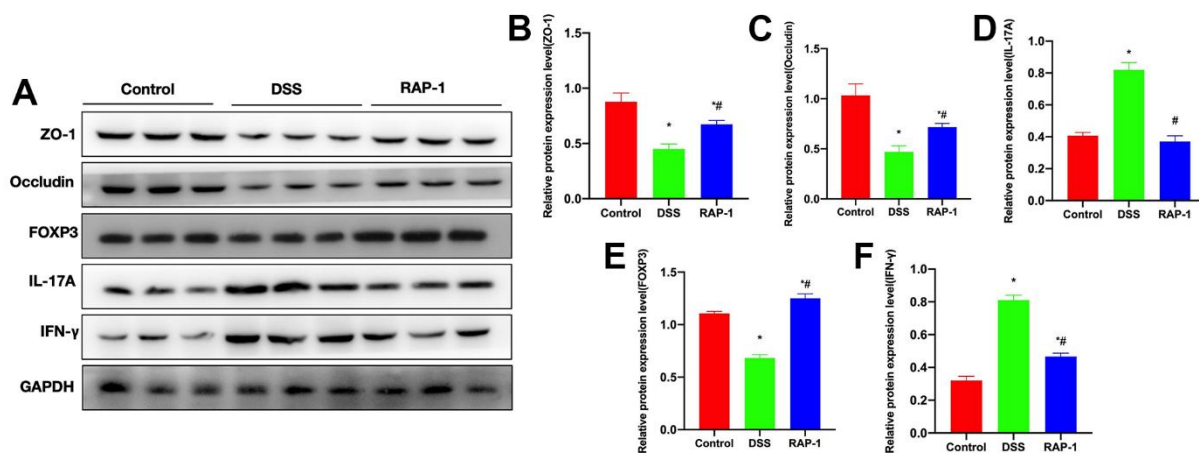

Figure 5. Relative protein expressions (n= 3). (**A**–**F**) DSS group exhibited downregulations of ZO-1, Occludin and FOXP3, whereas upregulations of IL-17A and IFN-γ. RAP1 could elevate the ZO-1, Occludin and FOXP3 levels, and lower the IL-17A and IFN-γ levels. *P< 0.05 vs. Control; #P< 0.05 vs. DSS.

enlargement of spleen, the foremost immune organ of the body, and relative reduction of thymus (spleen and thymus indices). RAP1 could mitigate intestinal inflammation, lower DAI score, ameliorate colon histopathological injury and reduce inflammatory cell infiltration, so that the thymus and spleen indices tended to be normal. These results suggested that RAP1 has certain therapeutic effects on the symptoms, tissue mucosa and immune response of colitis mice. In the intestinal tracts of patients with colitis, abnormal immune cell responses lead to entry of normal symbiotic flora and dietary antigens to the laminae propria. After activation of the host's innate immune system, the antigen presenting cells (APCs) induce T0 cell activation [11], resulting in differentiation of CD4+ T cells into Th1 and Th17 cells to produce more pro-inflammatory cytokines [12], while causing reduction of anti-inflammatory cytokines secreted by Tregs [13]. Under the action of APC, IL-12 is produced to promote the Th1 differentiation [14], and Th1 cells express transcriptional factors T-BET and IFN-γ. IFN-γ acts on CD4+ T cells, activates STAT1 signal, and promotes substantial expression of T-BET jointly with the signaling pathway downstream of TCR, thereby forming a positive feedback to synergistically promote the expression of IFN-γ [15]. Besides, IFN-γ can stimulate the production of chemokines like CCL3, CCL4 and CCL5 at the inflammatory site and, in the meantime, chemokine receptors like CCR5 and CXCR3 are also expressed on the Th1 surface, which are recruited to the inflammatory site after binding with respective ligands to exert a role, ultimately leading to the Th1/Th2 imbalance [16]. Th17 cells, which are differentiated from CD4+ T cells stimulated by TGF-β and IL-6, produce pro-inflammatory cytokines including IL-17, IL-21, IL-22, IL-23 and IL-25 [17]. IL-17, as a crucial pro-inflammatory cytokine, stimulates the secretion of TNF-α, IL-1β, IL-6 and IFN-γ [18]. Besides, it can also recruit neutrophil release and disrupt the intestinal epithelial barrier, thereby inducing intestinal inflammatory response [19, 20]. Tregs maintain intestinal homeostasis by secreting anti-inflammatory cytokines IL-10 and TGF-β. As an anti-inflammatory cytokine, TGF-β1 can inhibit disease progression and promote intestinal epithelial repair by regulating the immune response. IL-6, a pleiotropic cytokine involved in immune regulation and inflammation, can promote the differentiation of Th1, Th2 and Th17 cells and induce the T cell subsets to produce more pro-inflammatory cytokines [21, 22]. In this study, RAP1 exerted its anti-inflammatory role by inhibiting the secretion of pro-inflammatory TNF-α, IL-1β, IL-6, IL-17 and IFN-γ, while promoting the expression of TGF-β. Research has found that the intestinal antigens abnormally activate the immune system persistently, producing substantial inflammatory cytokines and inflammatory mediators, which induce apoptosis of intestinal epithelial cells by damaging them, thereby affecting the expression and distribution of tight junction proteins between epithelial cells and disrupting the tight junctions between epithelial cells. Meanwhile, the mucin production is inhibited and the mucus layer on epithelial cell surface is damaged, ultimately resulting in the compromise of intestinal mucosal barrier. According to the findings of this study, RAP1 can promote the ZO-1 and Occludin expressions in the intestinal tract of colitis mice, and facilitate the significant recovery of intestinal epithelial structure.

CONCLUSIONS

We isolated and identified a polypeptide RAP1 from Rhizoma Alismatis, which can regulate intestinal inflammation by modulating the intestinal cellular immunity in colitis, elevating the proportion of Tregs and lowering the proportions of inflammatory Th1 and Th17 cells. It can also reduce the expression of intestinal inflammatory cytokines. RAP1 has potential as a novel therapeutic polypeptide for colitis.

AUTHOR CONTRIBUTIONS

Zhongmei He, Tianyuan Liu: Responsible for experimental operations, including peptide extraction, separation, identification, and animal experiments; Rui Du; Xiaowei Dai, Honyan Pei: Responsible for analyzing experimental results and creating charts; Qiaobing Guan, Shuiliang Ruan, Shasha Wu: Responsible for providing funding for the project, writing and revising papers.

ACKNOWLEDGMENTS

CONFLICTS OF INTEREST

The authors declare that they have no conflicts of interest.

ETHICAL STATEMENT AND CONSENT

The mouse experiments were approved by the Ethics Committee of Jiaxing University, and carried out in line with the Guide for the Care and Use of Laboratory Animals. NO.JUMC2022-131.

REFERENCES

1. Yan P, Wei Y, Wang M, Tao J, Ouyang H, Du Z, Li S, Jiang H. Network pharmacology combined with metabolomics and lipidomics to reveal the hypolipidemic mechanism of Alismatis rhizoma in hyperlipidemic mice. Food Funct. 2022; 13:4714–33.
https://doi.org/10.1039/d1fo04386b PMID:35383784

2. Jia L, Zhang M, Wang P, Wang L, Lei P, Du R, Han L, Zhang P, Wang Y, Jiang M. Alismatis Rhizoma methanolic extract-Effects on metabolic syndrome and mechanisms of triterpenoids using a metabolomic and lipidomic approach. Front Pharmacol. 2022; 13:983428.
https://doi.org/10.3389/fphar.2022.983428 PMID:36160458

3. Bailly C. Pharmacological Properties and Molecular Targets of Alisol Triterpenoids from Alismatis Rhizoma. Biomedicines. 2022; 10:1945.
https://doi.org/10.3390/biomedicines10081945 PMID:36009492

4. Zhang LL, Xu W, Xu YL, Chen X, Huang M, Lu JJ. Therapeutic potential of Rhizoma Alismatis: a review on ethnomedicinal application, phytochemistry, pharmacology, and toxicology. Ann N Y Acad Sci. 2017; 1401:90–101.
https://doi.org/10.1111/nyas.13381 PMID:28662316

5. Jia XK, Huang JF, Huang XQ, Li XY, Huang MQ, Zhu HC, Li GP, Lan ML, Yu ZW, Xu W, Wu SS. Alismatis Rhizoma Triterpenes Alleviate High-Fat Diet-Induced Insulin Resistance in Skeletal Muscle of Mice. Evid Based Complement Alternat Med. 2021; 2021:8857687.
https://doi.org/10.1155/2021/8857687 PMID:33623531

6. Dai M, Li S, Shi Q, Xiang X, Jin Y, Wei S, Zhang L, Yang M, Song C, Huang R, Jin S. Changes in Triterpenes in Alismatis rhizoma after Processing Based on Targeted Metabolomics Using UHPLC-QTOF-MS/MS. Molecules. 2021; 27:185.
https://doi.org/10.3390/molecules27010185 PMID:35011422

7. Yan JB, Luo MM, Chen ZY, He BH. The Function and Role of the Th17/Treg Cell Balance in Inflammatory Bowel Disease. J Immunol Res. 2020; 2020:8813558.
https://doi.org/10.1155/2020/8813558 PMID:33381606

8. Larabi A, Barnich N, Nguyen HTT. New insights into the interplay between autophagy, gut microbiota and inflammatory responses in IBD. Autophagy. 2020; 16:38–51.
https://doi.org/10.1080/15548627.2019.1635384 PMID:31286804

9. Chang Y, Zhai L, Peng J, Wu H, Bian Z, Xiao H. Phytochemicals as regulators of Th17/Treg balance in inflammatory bowel diseases. Biomed Pharmacother. 2021; 141:111931.
https://doi.org/10.1016/j.biopha.2021.111931 PMID:34328111

10. Chen Y, Zhang P, Chen W, Chen G. Ferroptosis mediated DSS-induced ulcerative colitis associated with Nrf2/HO-1 signaling pathway. Immunol Lett. 2020; 225:9–15.
https://doi.org/10.1016/j.imlet.2020.06.005 PMID:32540488

11. Lin R, Ma C, Fang L, Xu C, Zhang C, Wu X, Wu W, Zhu R, Cong Y, Liu Z. TOB1 Blocks Intestinal Mucosal Inflammation Through Inducing ID2-Mediated Suppression of Th1/Th17 Cell Immune Responses in IBD. Cell Mol Gastroenterol Hepatol. 2022; 13:1201–21.
https://doi.org/10.1016/j.jcmgh.2021.12.007 PMID:34920145

12. Lin R, Wu W, Chen H, Gao H, Wu X, Li G, He Q, Lu H, Sun M, Liu Z. GPR65 promotes intestinal mucosal Th1 and Th17 cell differentiation and gut inflammation through downregulating NUAK2. Clin Transl Med. 2022; 12:e771.
https://doi.org/10.1002/ctm2.771 PMID:35343079

13. Jiang P, Zheng C, Xiang Y, Malik S, Su D, Xu G, Zhang M. The involvement of TH17 cells in the pathogenesis of IBD. Cytokine Growth Factor Rev. 2023; 69:28–42.
https://doi.org/10.1016/j.cytogfr.2022.07.005 PMID:35871978

14. Lee JY, Hall JA, Kroehling L, Wu L, Najar T, Nguyen HH, Lin WY, Yeung ST, Silva HM, Li D, Hine A, Loke P, Hudesman D, et al. Serum Amyloid A Proteins Induce Pathogenic Th17 Cells and Promote Inflammatory Disease. Cell. 2020; 180:79–91.e16.
https://doi.org/10.1016/j.cell.2019.11.026 PMID:31866067

15. Feroz SH, Ahmed A, Muralidharan A, Thirunavukarasu P. Comparison of the Efficacy of the Various Treatment Modalities in the Management of Perianal Crohn's Fistula: A Review. Cureus. 2020; 12:e11882.
https://doi.org/10.7759/cureus.11882 PMID:33415035

16. Chen YF, Zheng JJ, Qu C, Xiao Y, Li FF, Jin QX, Li HH, Meng FP, Jin GH, Jin D. Inonotus obliquus polysaccharide ameliorates dextran sulphate sodium

induced colitis involving modulation of Th1/Th2 and Th17/Treg balance. Artif Cells Nanomed Biotechnol. 2019; 47:757–66.
https://doi.org/10.1080/21691401.2019.1577877
PMID:30856346

17. Ma C, Wu W, Lin R, Ge Y, Zhang C, Sun S, Cong Y, Li X, Liu Z. Critical Role of CD6highCD4+ T Cells in Driving Th1/Th17 Cell Immune Responses and Mucosal Inflammation in IBD. J Crohns Colitis. 2019; 13:510–24.
https://doi.org/10.1093/ecco-jcc/jjy179
PMID:30395204

18. Moschen AR, Tilg H, Raine T. IL-12, IL-23 and IL-17 in IBD: immunobiology and therapeutic targeting. Nat Rev Gastroenterol Hepatol. 2019; 16:185–96.
https://doi.org/10.1038/s41575-018-0084-8
PMID:30478416

19. Hang S, Paik D, Yao L, Kim E, Trinath J, Lu J, Ha S, Nelson BN, Kelly SP, Wu L, Zheng Y, Longman RS, Rastinejad F, et al. Bile acid metabolites control TH17 and Treg cell differentiation. Nature. 2019; 576:143–8.
https://doi.org/10.1038/s41586-019-1785-z
PMID:31776512

20. Fauny M, Moulin D, D'Amico F, Netter P, Petitpain N, Arnone D, Jouzeau JY, Loeuille D, Peyrin-Biroulet L. Paradoxical gastrointestinal effects of interleukin-17 blockers. Ann Rheum Dis. 2020; 79:1132–8.
https://doi.org/10.1136/annrheumdis-2020-217927
PMID:32719044

21. Ihara S, Hirata Y, Koike K. TGF-β in inflammatory bowel disease: a key regulator of immune cells, epithelium, and the intestinal microbiota. J Gastroenterol. 2017; 52:777–87.
https://doi.org/10.1007/s00535-017-1350-1
PMID:28534191

22. Sedda S, Marafini I, Dinallo V, Di Fusco D, Monteleone G. The TGF-β/Smad System in IBD Pathogenesis. Inflamm Bowel Dis. 2015; 21:2921–5.
https://doi.org/10.1097/MIB.0000000000000542
PMID:26230862